# Variability of apatite fission-track annealing kinetics: II. Crystallographic orientation effects

RAYMOND A. DONELICK,[1,*] RICHARD A. KETCHAM,[2,†] AND WILLIAM D. CARLSON[2]

[1]Department of Geology and Geophysics, Rice University, Houston, Texas 77005, U.S.A.
[2]Department of Geological Sciences, University of Texas at Austin, Austin, Texas 78712, U.S.A.

## ABSTRACT

A method is presented that permits the length of any horizontal, confined fission-track inclined at a specified angle to the crystallographic *c* axis in apatite to be converted to an equivalent track length parallel to the crystallographic *c* axis. The model is based on the results of annealing experiments for six selected apatites (five calcian fluorapatites and Durango apatite) representing a subset of the 15 total apatite specimens studied. An iterative process of calculation is required to project fission-track lengths onto the *c* axis and computer source code implementing the solution to this problem is presented.

This method of projecting apatite fission-track lengths onto the crystallographic *c* axis is shown to remove effectively fission-track length variation within single fission-track populations due to anisotropic track-length reduction for all 15 apatites studied. In addition, a model is developed that offers predictions that closely reproduce published experimental data concerning the relationship between fission-track density (etched fission tracks per unit area of apatite surface) and the arithmetic mean fission-track length. Finally, it is shown that natural fission-track populations exhibit fission-track length anisotropy similar to that of fission-track populations created and annealed in the laboratory. This observation implies that the same process by which apatite fission tracks anneal in the laboratory is responsible for annealing of apatite fission tracks in the geological environment.

## INTRODUCTION

Laboratory annealing experiments have shown consistently that fission tracks oriented at high angles to the crystallographic *c* axis in hexagonal apatites are, on average, shorter than fission tracks at low angles to the *c* axis, even in relatively unannealed apatites (Green et al. 1986; Donelick et al. 1990; Donelick 1991; Crowley et al. 1991) and that the anisotropy of fission-track length in apatite increases as the degree of annealing increases (Fig. 1). The model of Donelick (1991) attempts to quantify this effect, proposing that etched lengths of a single population of fission tracks in apatite are distributed about an ellipse in *c* axis parallel crystallographic planes, with the mean track length parallel to the *c* axis ($l_c$) being greater than the mean track length perpendicular to the *c* axis ($l_a$) in all cases. As the degree of fission-track annealing increases and the arithmetic mean track length ($l_m$) decreases, $l_c$ becomes increasingly greater than $l_a$. The divergence of $l_a$ from $l_c$ leads directly to an increased spread in the track-length distribution about $l_m$ until at high levels of annealing the standard deviation about $l_m$ approaches 2 μm or more. The elliptical model of Donelick (1991) works well until the mean fission-track length falls below ~11 μm (corresponding to a reduced length of ~0.65), after which fission tracks at high angles to the *c* axis begin to undergo accelerated length reduction. While of no large

consequence for the experimental determination of $l_m$, the anisotropy of fission-track lengths in apatite can complicate the interpretation of track-length data from the geological environment, in which a limited number of fission-track lengths is used in most cases to reconstruct a complete time-temperature history (e.g., Green et al. 1989; Corrigan 1991; Crowley 1993; Willett 1997). The experimental data of Carlson et al. (1999, this volume) offers a unique opportunity to construct a model for use in projecting natural fission-track lengths to a common crystallographic orientation in apatite as suggested by Carlson (1990, p. 1135). Ketcham et al. (1999, this volume) use this model to provide fission-track length calibrations specific to fission tracks oriented parallel to the crystallographic *c* axis.

## SAMPLE DETAILS AND EXPERIMENTAL METHODS

Fifteen apatites spanning a wide range of chemical compositions were used in this study (Table 1; also see Table 1 and Appendix Table 1 of Carlson et al. 1999, this volume). Full details concerning the preparation, treatment, and analysis of the apatites for these experiments are provided in Carlson et al. (1999, this volume). Individual track lengths and angles to the crystallographic *c* axis were measured using a digitizing tablet interfaced with a personal computer. Positioning of the digitizer cursor within the optical field of view was aided by projection of the image of an LED light attached to the cursor onto the microscope field of view. The digitizer surface was calibrated for length measurement using a 600 lines/mm diffraction grating. The length of each fission track and its angle to the crystallographic *c* axis were computed from three digitized points per track, one at each end of the track and one

*Current Address: Department of Geology and Geological Engineering, University of Idaho, Moscow, Idaho 83844, U.S.A.
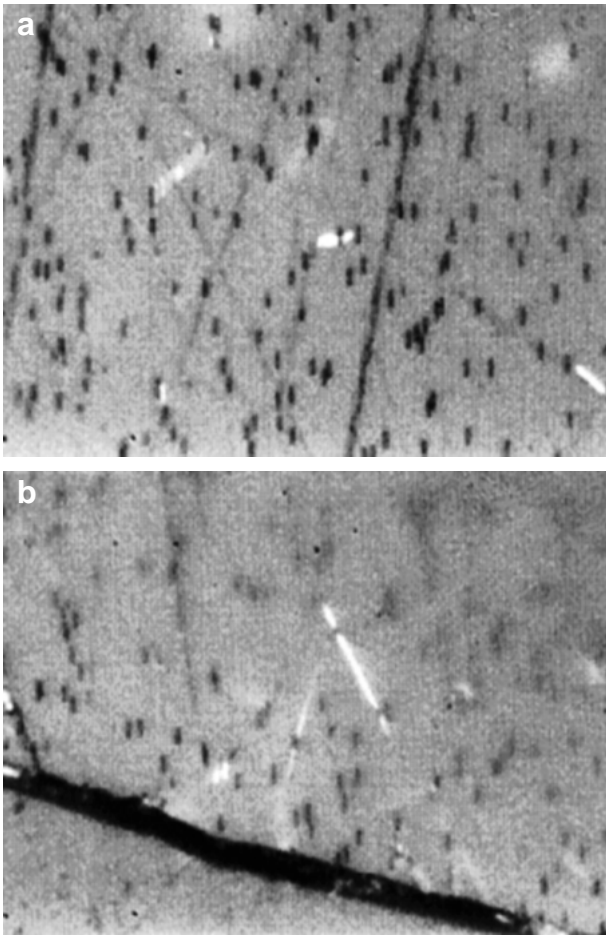†E-mail: richk@maestro.geo.utexas.edu

**FIGURE 1.** Reflected light photomicrographs of etched, confined TINT fission tracks (center of the fields of view) measured for apatite RN, run 67. (**a**) Length 2.97 μm, inclined 80° from the crystallographic *c* axis. (**b**) Length 11.45 μm inclined 22° to the *c* axis. The *c* axis is oriented vertically in both photomicrographs and each is approximately 50 μm across the horizontal direction.

**TABLE 1.** Summary list of the 15 apatite specimens used in this study

| Apatite | Locality | $D_{par}$ (μm) | $D_{per}$ (μm) | Cl (apfu) |
|---|---|---|---|---|
| AY | Ayacucho, Peru | 1.95(15) | 0.42(10) | 0.24 |
| B2 | Bamble, Norway | 4.58(32) | 2.21(21) | 0.87 |
| B3 | Bamble, Norway | 4.99(29) | 2.49(24) | 1.87 |
| DR | Durango, Mexico | 1.83(13) | 0.43(13) | 0.12 |
| FC | Fish Canyon, Colorado | 2.43(21) | 0.83(11) | 0.24 |
| HS | Holly Springs, Georgia | 3.00(29) | 1.81(10) | 0.10 |
| KP | Kola Peninsula, Russia | 2.06(19) | 0.64(10) | 0.00 |
| OL | Otter Lake, Quebec | 2.35(12) | 0.56(12) | 0.01 |
| PC | Portland, Connecticut | 2.15(13) | 0.72(09) | 0.00 |
| PQ | Panasquiera, Portugal | 1.59(12) | 0.34(06) | 0.00 |
| RN | Renfrew Co., Ontario | 1.65(13) | 0.41(04) | 0.01 |
| SC | Silver Crater, Ontario | 1.71(17) | 0.42(11) | 0.00 |
| TI | Old Port, Pennsylvania | 2.45(20) | 0.80(10) | 0.17 |
| UN | Unknown | 1.89(12) | 0.44(12) | 0.02 |
| WK | Wakefield, Ontario | 1.87(16) | 0.47(11) | 0.01 |

*Notes:* $D_{par}$ = mean maximum diameter of fission-track etch figures parallel to the crystallographic *c* axis; $D_{per}$ = mean maximum diameter of fission-track etch figures perpendicular to the crystallographic *c* axis; Cl apfu determined by electron microprobe and calculated assuming $Ca_{10}(PO_4)_6[F,Cl,OH]_2$. The numbers in parentheses indicate one standard deviation in significant figures.

along the crystallographic *c* axis from the second (Fig. 2). The precision of each track length and angle to the crystallographic *c* axis is approximately ±0.15 μm and ±2°, respectively (Donelick 1991).

## CONSTRUCTION OF THE *C*-AXIS PROJECTION MODEL

### General

The 15 apatites studied by Carlson et al. (1999, this volume) exhibit a wide range of anion and cation substitutions and, because many of these apatite compositions are quite rare or unusual, the model presented below is based on results obtained for a subset of six apatites. These apatites consist of five near-end-member calcian fluorapatites (PQ, RN, SC, UN, and WK), the most common variety of apatite encountered in the geological environment, all of which exhibit similar annealing characteristics. Also included in the subset is the Durango (DR) apatite that has approximately 0.12 apfu Cl; it is included because it has been widely studied experimentally (e.g., Green et al. 1986; Green 1988) and it is a fair representative of slightly chlorine-rich apatites, which are also quite common in the geological environment. Of the six apatites, results from DR and RN dominate this analysis, as they were measured in approximately 70 experiments each as opposed to 12 each for the others. This set of apatites is referred to in the subsequent analysis as the *six selected apatites*. Inclusion of the nine remaining apatites introduces additional scatter to the data upon which the fission-track length *c* axis projection model is based. An effort was made to discover systematic behavior on the basis of apatite etching characteristics (parameters $D_{par}$ and $D_{per}$ in Table 1; Burtner et al. 1994; Donelick (1993, 1995) and a variety of compositional parameters including chlorine content (parameter Cl apfu in Table 1) but no clear trends are apparent. Regardless, it is shown below that the *c* axis projection model developed on the basis of the six selected apatites successfully characterizes the fission-track length vs. crystallographic orientation relationship of 7 of the 9 remaining apatites as well.

Etchable length reduction of fission tracks in apatite occurs in two stages (e.g., Green et al. 1986). At relatively low degrees of annealing ($l_m$ > approximately 11 μm), fission-track



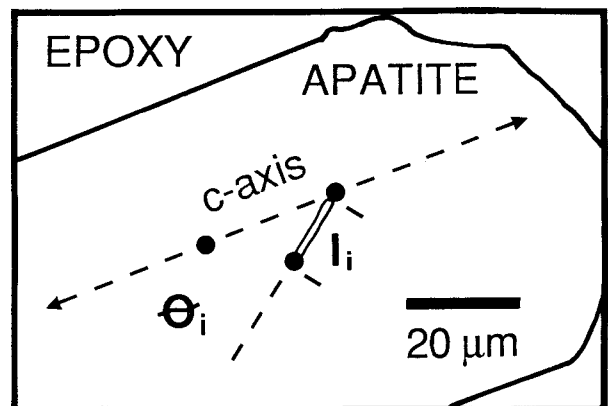**FIGURE 2.** Fission-track length ($l_i$) and inclination angle ($\theta_i$) to the crystallographic *c* axis.

lengths are approximately uniformly distributed about an ellipse with respect to track angle to the crystallographic $c$ axis (Fig. 3a–c). Donelick (1991) demonstrated this notion and showed that the standard deviation about the mean fission-track length at any given crystallographic orientation in Tioga apatite is approximately constant at 0.75 μm at relatively low degrees of annealing. At relatively high degrees of annealing ($l_m$ < approximately 11 μm), the ellipse about which the fission tracks are distributed collapses, with fission tracks at relatively high angles to the crystallographic $c$ axis experiencing systematic, accelerated length reduction (Fig. 3d–f). As the degree of annealing increases, the initiation of the collapse of the ellipses rotates toward the $c$ axis. Previous studies, notably Green et al. (1986), have attributed accelerated length reduction to a process of fission-track segmentation, with track segments becoming interrupted by zones of annealed crystal through which the chemical etchant cannot easily penetrate. It is noteworthy that the etched fission track shown by Green et al. (1986, their Fig.

11) exhibits a morphology characterized by sharply tapered ends that is only seen in tracks that are nearly perpendicular to the crystallographic $c$ axis. Furthermore, this fission-track morphology is observed *throughout* the range of annealing (Fig. 4), in many cases causing fission tracks oriented nearly perpendicular to the crystallographic $c$ axis to appear under-etched relative to their counterparts at other orientations. Given these observations, it is unclear whether fission-track segmentation, as described by Green et al. (1986), is responsible for the progressive collapse of the fission-track length ellipses or if some other process that affects fission-track etching velocities is responsible.

The two stages of etchable fission-track length reduction in apatite described above lead to the necessity of distinguishing between two types of individual confined fission tracks: (1) *elliptical-model fission track*, one of a population of fission-tracks that are approximately uniformly distributed about an ellipse or part of an ellipse; and (2) *accelerated-length-reduc-*
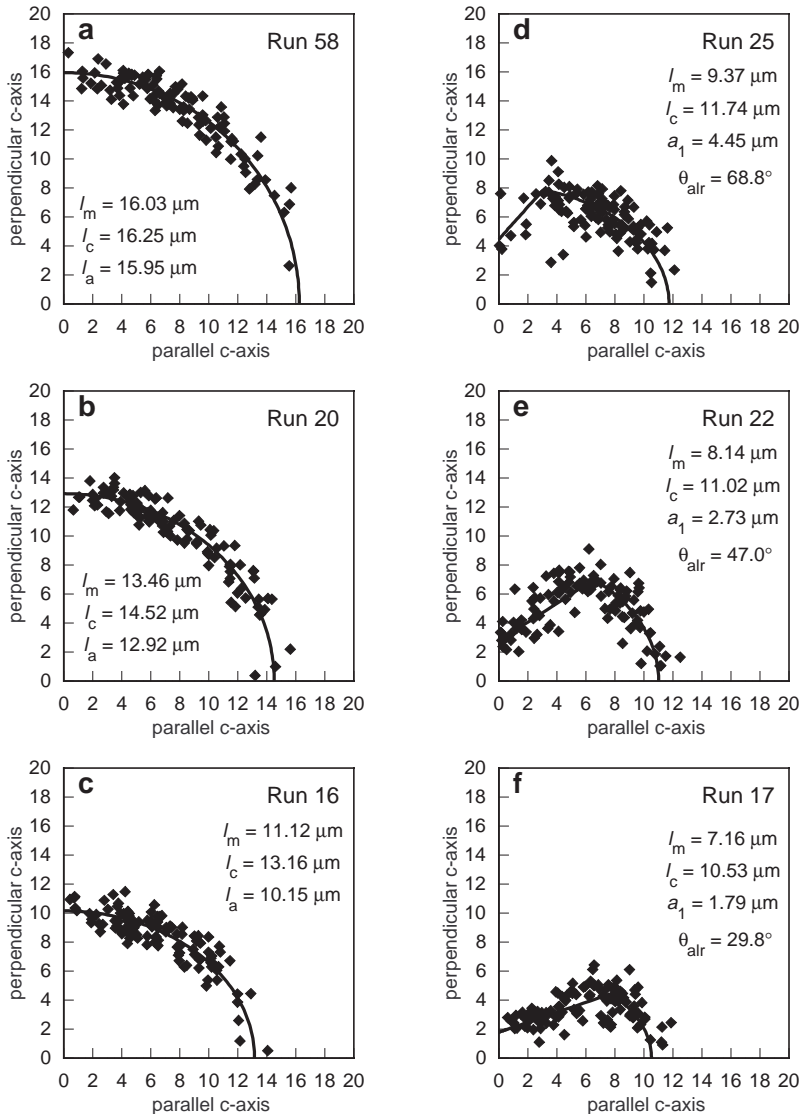


**FIGURE 3.** Polar coordinate plots of the fission-track lengths measured for the following runs: (**a**) DR58, (**b**) DR20, (**c**) DR16, (**d**) DR252, (**e**) DR22, (**f**) DR17.

*tion fission track*, a fission track that has experienced systematic accelerated length reduction that, in polar coordinate space, causes its length value to plot well inside the ellipse passing through the accompanying elliptical-model fission tracks.

The model of Donelick (1991) is expanded upon below based on absolute fission-track length for the six selected apatites yielding a detailed model of fission-track length distribution vs. crystallographic orientation for all degrees of annealing studied by Carlson et al. (1999, this volume). Reduced fission-track length (e.g., Laslett et al. 1987; Ketcham et al. 1999, this volume) was considered and the results are very similar to those based on absolute fission-track length. However, absolute fission-track length was preferred due to the large errors associated with estimates of initial $l_c$ and $l_a$ values. The overall $c$-axis projection model was arrived at as follows. (1) *Distinguish between elliptical-model fission tracks and accelerated-length-reduction fission tracks*. For each experiment that exhibits evidence of accelerated length reduction, a threshold angle to
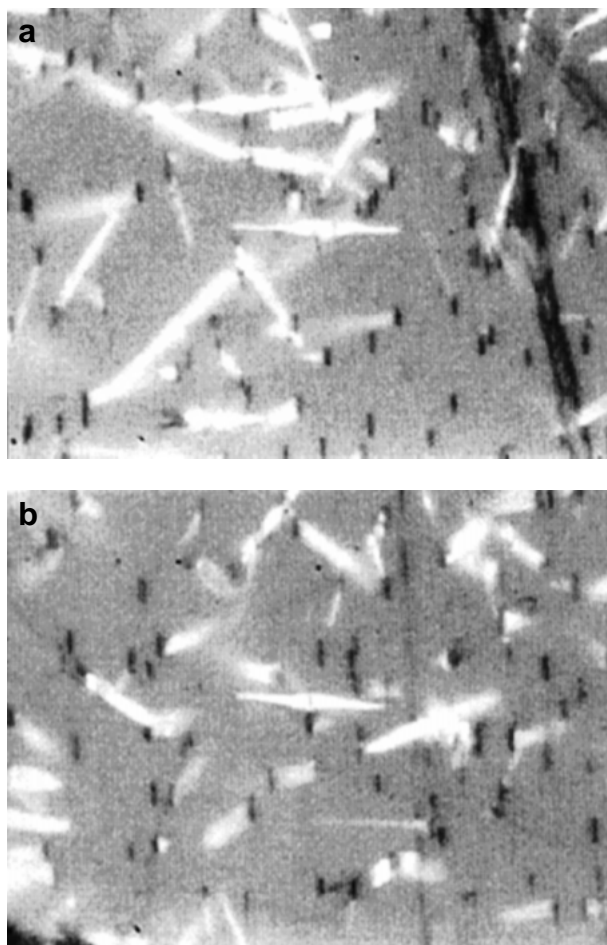
**TABLE 2.** Fitted parameters for the 36 experiments of Carlson et al. (this volume) that exhibit evidence of accelerated length reduction

| Apatite | Run | $l_c$ (µm) | $l_a$ (µm) | $\theta_{alr}$ (degrees) |
|---|---|---|---|---|
| AY | 63 | 11.42 | 8.42 | 58.6 |
| AY | 66 | 10.96 | 6.93 | 39.0 |
| B3 | 26 | 11.76 | 6.77 | 30.2 |
| B3 | 28 | 11.96 | 8.56 | 47.9 |
| B3 | 31 | 11.93 | 7.20 | 30.4 |
| B3 | 47 | 11.59 | 7.33 | 32.6 |
| DR | 17 | 10.53 | 6.57 | 29.8 |
| DR | 22 | 11.02 | 8.70 | 47.0 |
| DR | 25 | 11.74 | 8.14 | 68.8 |
| DR | 46 | 11.43 | 8.02 | 49.5 |
| DR | 63 | 11.94 | 8.43 | not estimated |
| DR | 66 | 10.88 | 7.56 | 34.3 |
| HS | 16 | 11.01 | 8.38 | 63.3 |
| HS | 21 | 9.10 | 6.37 | 25.5 |
| HS | 24 | 9.72 | 6.53 | 38.2 |
| HS | 48 | 9.80 | 7.15 | 30.4 |
| HS | 49 | 11.38 | 9.33 | 58.2 |
| HS | 67 | 10.26 | 3.49 | 14.3 |
| HS | 71 | 9.53 | 6.77 | not estimated |
| OL | 63 | 9.41 | 8.15 | 12.9 |
| OL | 71 | 11.56 | 9.40 | 55.3 |
| PQ | 63 | 9.97 | 4.90 | 19.6 |
| PQ | 71 | 12.33 | 9.69 | 63.9 |
| RN | 16 | 12.17 | 8.49 | 61.0 |
| RN | 24 | 12.71 | 8.63 | 63.5 |
| RN | 38 | 11.82 | 8.94 | 51.3 |
| RN | 46 | 9.88 | 1.53 | 21.8 |
| RN | 48 | 12.60 | 8.18 | 64.8 |
| RN | 67 | 12.35 | 7.80 | 58.5 |
| RN | 71 | 11.45 | 8.14 | 51.6 |
| SC | 63 | 9.31 | 5.26 | 17.1 |
| SC | 71 | 11.68 | 8.86 | 52.2 |
| UN | 63 | 9.51 | 5.73 | 18.4 |
| UN | 71 | 11.27 | 9.99 | 54.6 |
| WK | 63 | 9.81 | 4.81 | 27.1 |
| WK | 71 | 12.55 | 8.92 | 79.0 |

the crystallographic $c$ axis ($\theta_{alr}$) was determined above which accelerated length reduction begins to dominate. (2) *Characterize elliptical-model fission tracks*. For each experiment lacking evidence of accelerated length reduction, an ellipse was fit to all fission tracks measured (minus any observed outliers) yielding values of $l_c$ and $l_a$. For each experiment exhibiting accelerated length reduction, an ellipse was fit to all fission tracks measured (minus any observed outliers) that are oriented at an angle less than or equal to $\theta_{alr}$ yielding values of $l_c$ and $l_a$. An expression relating $l_c$ and $l_a$ was then obtained for all degrees of fission-track annealing studied. (3) *Characterize accelerated-length-reduction fission tracks*. For all experiments exhibiting evidence of accelerated length reduction, an expression relating $\theta_{alr}$ and $l_c$ was derived. For each such individual experiment, the lengths of accelerated-length-reduction fission tracks are distributed approximately about a line having a $c$ axis perpendicular intercept of $a_1$ and intersecting its accompanying ellipse at the point corresponding to $\theta_{alr}$. An expression relating $a_1$ and $\theta_{alr}$ was derived from all such experiments.

## Distinguish between elliptical-model fission tracks and accelerated-length-reduction fission tracks

Polar coordinate plots, like those shown in Figure 3, were constructed for each individual annealing experiment. The experiments were then segregated based on whether or not they

**FIGURE 4.** Reflected light photomicrographs of etched, confined TINT fission tracks (center of the fields of view) measured for apatite RN. (**a**) Run 0 (the initial condition), length 13.17 µm inclined 87° to the crystallographic $c$ axis. (**b**) Run 8, length 11.93 µm inclined 80° to the $c$ axis. The $c$ axis is oriented vertically in both photomicrographs and each is approximately 50 µm across the horizontal direction.

exhibited evidence of accelerated length reduction at relatively high angles to the crystallographic $c$ axis. A total of 36 experiments exhibit evidence of accelerated length reduction (Table 2). For each, a threshold angle ($\theta_{alr}$) was defined as the angle to the crystallographic $c$ axis above which a large proportion (>30–50%) of fission tracks start to show excessive shortening. The precise value was assigned based on the angle of the first fission track in the accelerated-length-reduction population. In experiments that were measured both with and without the use of $^{252}$Cf-irradiation (see Appendix Tables 2 and 3[1] of Carlson et al. 1999, this volume), only the measurements that employed $^{252}$Cf-irradiation were used for determination of $\theta_{alr}$ because they offer a larger number of track lengths measured over a greater range of angles to the crystallographic $c$ axis. In general, the transition across $\theta_{alr}$ from elliptical-model fission tracks to accelerated-length-reduction fission tracks is fairly sudden (Fig. 3d–f), typically occurring over a 5–10° span. However, owing to the limited number of fission tracks with angles in the neighborhood of $\theta_{alr}$, the value of $\theta_{alr}$ has an undetermined error, probably in the range of 5–10°.

## Characterize elliptical-model fission tracks

Elliptical-model fission tracks were characterized as follows. (1) For each experiment that does not exhibit evidence of accelerated length reduction, an ellipse was fit to all fission-track lengths measured, minus a few outliers on its polar coordinate plot, using the method of Donelick (1991). Of the 38,378 fission tracks measured in these experiments for the 15 apatites studied by Carlson et al. (1999, this volume; not including re-measurement of experiments that had initially been $^{252}$Cf-irradiated), a total of 62 were judged to be outliers and deleted (0.16% of the total; < 1 track per 5 individual experiments). The most poorly behaved apatites are FC, for which 10 of 1308 fission tracks were outliers, and PQ, for which 13 of 976 were outliers. (2) For each experiment that exhibits evidence of accelerated length reduction, an ellipse was fit to only the elliptical-model fission tracks oriented at an angle ≤$\theta_{alr}$ to the crystallographic $c$ axis, minus any outliers on its polar coordinate plot (0–3 tracks per experiment). Of the 3346 fission tracks measured in these experiments for the 15 apatites studied by Carlson et al. (1999, this volume; not including re-measurement of experiments that had initially been $^{252}$Cf-irradiated), 61 were deleted (1.82%; <2 tracks per individual experiment). Donelick (1991) demonstrated that this method of fitting ellipses to angular subsets of fission tracks agrees well with ellipses fitted to complete data sets. However, this procedure can produce incorrect results if there are too few fission-track lengths along too limited an angular range. Furthermore, the separation of elliptical-model fission tracks from accelerated-length-reduction tracks may not be straightforward in all cases.

---

[1]For a copy of Appendix Tables 1–3 of Carlson et al. (1999, this volume), document item AM-99-023, contact the Business Office of the Mineralogical Society of America (see inside front cover of recent issue) for price information. Deposit items may also be available on the American Mineralogist web site (http://www.minsocam.org or current web address).
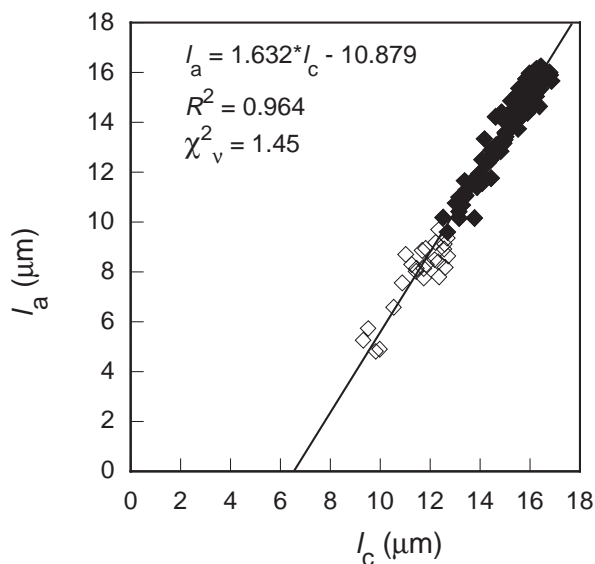


**FIGURE 5.** Plot of $l_a$ vs. $l_c$ for the six selected apatites. Filled diamond = experiments without accelerated length reduction. Open diamond = experiments with accelerated length reduction.

Fitted values of $l_c$ and $l_a$ were obtained for the 36 experiments exhibiting evidence of accelerated length reduction (Table 2); however, several of these values are probably not reliable, for the reason listed above. All of the these experiments with fitted values we judged reliable are indicated by an asterisk (*) in Appendix Tables 2 and 3 of Carlson et al. (1999, this volume); the experiments for which fitted parameters were based on inadequate data are indicated by a double asterisk (**). Figure 5 is a plot of $l_c$ vs. $l_a$ for the six selected apatites. The solid and open symbols indicate experiments that do and do not exhibit evidence of accelerated length reduction, respectively. A line was fitted to the data plotted in Figure 5 using $\chi^2$ minimization and taking into account the estimated errors in both $l_c$ and $l_a$. The expression is:

$$l_a = 1.632\, l_c - 10.879;\ R^2 = 0.964;\ \chi^2_v = 1.63 \qquad (1)$$

## Characterize accelerated-length-reduction fission tracks

Figure 6 is a plot of $\theta_{alr}$ vs. $l_c$ for the six selected apatites. Importantly, $\theta_{alr}$ exhibits a strong tendency to decrease as $l_c$ decreases. Qualitatively, this means that as $l_c$ decreases, the threshold for the collapse of the ellipse swings closer to the crystallographic $c$ axis. The relation between $\theta_{alr}$ and $l_c$ is estimated as:

$$\theta_{alr} = 0.304 \exp(0.439\, l_c). \qquad (2)$$

One implication of Equation 2 is that accelerated length reduction is not expected for $l_c$ values >12.96 μm (the value where $\theta_{alr}$ equals 90°). Considering this further, the choice of the exponential form of Equation 2 was made for the following reasons. First, when a linear expression is used, the $l_c$ corresponding to $\theta_{alr} = 90°$ is greater than 13.5 μm, implying that

there would be evidence of accelerated length reduction in fission-track populations having this $l_c$ value. In fact, no experiments in the data of Carlson et al. (1999, this volume) exhibit evidence of accelerated length reduction when $l_c > 12.8$ μm, and there are numerous experiments that lack evidence of accelerated length reduction when $l_c < 13.5$ μm (Table 2). Second, an exponential model is as simple as a linear model, insofar as it requires the fitting of only two free parameters. Third, the fact that Equation 2 does not permit the condition $\theta_{alr} = 0°$ is of no consequence, because the lowest $\theta_{alr}$ observed among the six selected apatites is 17.1°, and the lowest value overall is 12.9° (Table 2).

As shown in Figure 3d–f, the fission tracks that show accelerated length reduction for each individual experiment can be approximated by a line segment extending from the intersection of the fitted ellipse with angle $\theta_{alr}$ to the $c$-perpendicular axis. Given the parameters already specified, the only parameter that is necessary to define this line segment for an individual experiment is its $c$-perpendicular intercept, denoted $a_1$. Additionally, $a_1$ was assumed to be a linear function of $\theta_{alr}$ over the range of experiments exhibiting accelerated length reduction and Equations 1 and 2 above were assumed to be valid. The free parameters for the linear function relating $a_1$ and $\theta_{alr}$ for the six selected apatites were obtained by minimizing the misfit between the $c$-axis parallel projection of each accelerated-length-reduction fission track and the respective value of $l_c$. This was done using $\chi^2$ minimization, assuming errors proportional to the standard error of the fitted $c$ axis-parallel value, using techniques described in Appendix A of Ketcham et al. (1999, this volume). The resulting expression is

$$a_1 = 0.1035\ \theta_{alr} - 2.250. \qquad (3)$$

### The apatite fission-track length $c$-axis projection model

Equations 1 through 3 were used to construct the fission-track length $c$ axis projection model depicted in Figure 7, where each curve represents a selected pathway along which an individual fission-track length may be projected onto the crystallographic $c$ axis. An iterative solution to Equations 1 through 3 is necessary, as there is no analytical solution to the combination of these equations. The Appendix[1] provides a detailed summary of this iterative approach, a short computer program written in FORTRAN that implements this approach, and a table of example calculations.

### VERIFICATION OF THE MODEL

Figure 8 shows the residuals obtained by subtracting the mean $c$-axis parallel length for each experiment predicted by projecting each individual track using Equations 1 through 3 above from the corresponding fitted value for each experiment. The residuals for the six selected apatites shown in Figure 8a
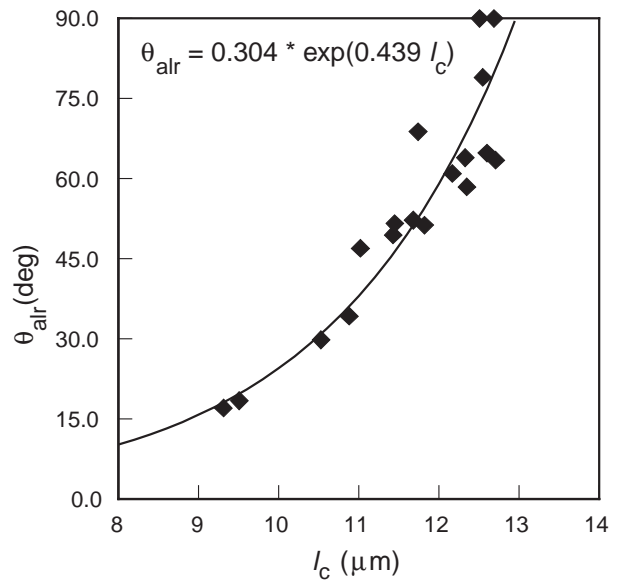
---

[1]For a copy of the Appendix, Document AM-99-019, contact the Business Office of the Mineralogical Society of America (see inside front cover of recent issue) for price information. Deposit items may also be available on the American Mineralogist web site (http://www.minsocam.org or current web address).



**FIGURE 6.** Plot of $\theta_{alr}$ vs. $l_c$ for the six selected apatites.

support the validity of the $c$-axis projection model; for modeled mean track lengths from 17 μm to 11 μm the mean residual is generally < 0.1 μm. For mean track lengths <11 μm the residual is generally negative, which may be due to the sparsity of experiments with such short mean lengths, or it may be a consequence of the simplifications inherent in the model. As shown in Figure 8b, the residuals for 7 of the remaining 9 apatites studied show behavior similar to that of the six selected apatites. The two most poorly behaved apatites are the hydroxyapatite HS and the strontian fluorapatite KP; both of these exhibit significant negative residuals (Fig. 8b). The poor behavior of HS and KP arises principally from a difference in the relation between the fitted values for $l_c$ and $l_a$. A re-calculation of Equation 1 specific to these two apatites gives the relation:

$$l_a = 1.293\ l_c - 5.218;\ R^2 = 0.974;\ \chi_v^2 = 2.40 \qquad (4)$$

The chemical compositions of these two apatites are quite unusual and rare (Carlson et al. 1999, this volume), and the current data set is insufficient to quantify with confidence how compositional variation affects the $l_c$ vs. $l_a$ relationship.

The residuals between $l_c$ and $l_{c,mod}$ were investigated over the full range of fission-track annealing studied and it was found that the residuals compare closely to the uncertainties in individual determinations of $l_{c,mod}$. We were thus unable to detect a significant error in the determination of $l_{c,mod}$ over and above the calculated standard error of $l_{c,mod}$ that requires propagation in subsequent modeling.

Figure 9 compares the standard deviation of measured fission track lengths ($\sigma_m$) about $l_m$ vs. the standard deviation of $c$-axis projected fission-track lengths ($\sigma_{c,mod}$) about $l_{c,mod}$ (Carlson et al. 1999, this volume, their Appendix Tables 2 and 3). The significant effect of the $c$-axis projection model depicted in Figure 9 is that it flattens the plot of $\sigma_{c,mod}$ vs. $l_{c,mod}$ (Fig. 9b) in comparison to the plot of $\sigma_m$ vs. $l_m$ (Fig. 9a).
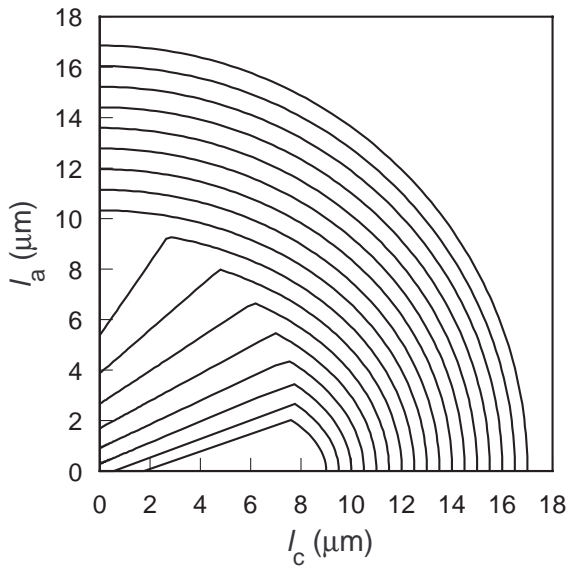
**FIGURE 7.** The apatite fission-track length *c*-axis projection model based on the six selected apatites.

## DISCUSSION

### Fission-track length observational bias

Laslett et al. (1982) presented a mathematical description of the probability of observing, and by extension measuring, confined fission-track lengths based on their physical attributes such as the lengths of the tracks themselves and the geometry of the etchant pathways. Their model holds that for apatites exhibiting a spectrum of fission-track lengths, shorter tracks are less likely to be etched and therefore measured than their longer counterparts. For an idealized situation where the etchant pathway has negligible width, the relative likelihood of etching, and subsequently measuring, any given track is proportional to its length. To date, no published studies have been presented that test the model of Laslett et al. (1982). Identifying fission tracks as either TINT (Track-IN-Track), TINCLE (Track-IN-CLEavage), or TINDEF (Track-IN-DEFect) fission tracks is important because, as Laslett et al. (1982) demonstrate, the probability of observing and measuring the full length of any given etched, confined fission track is a function of the width of the etchant pathway that the track of interest intersects.

The results of this study indicate that the probability of observing a fission track and measuring its length is also depen-
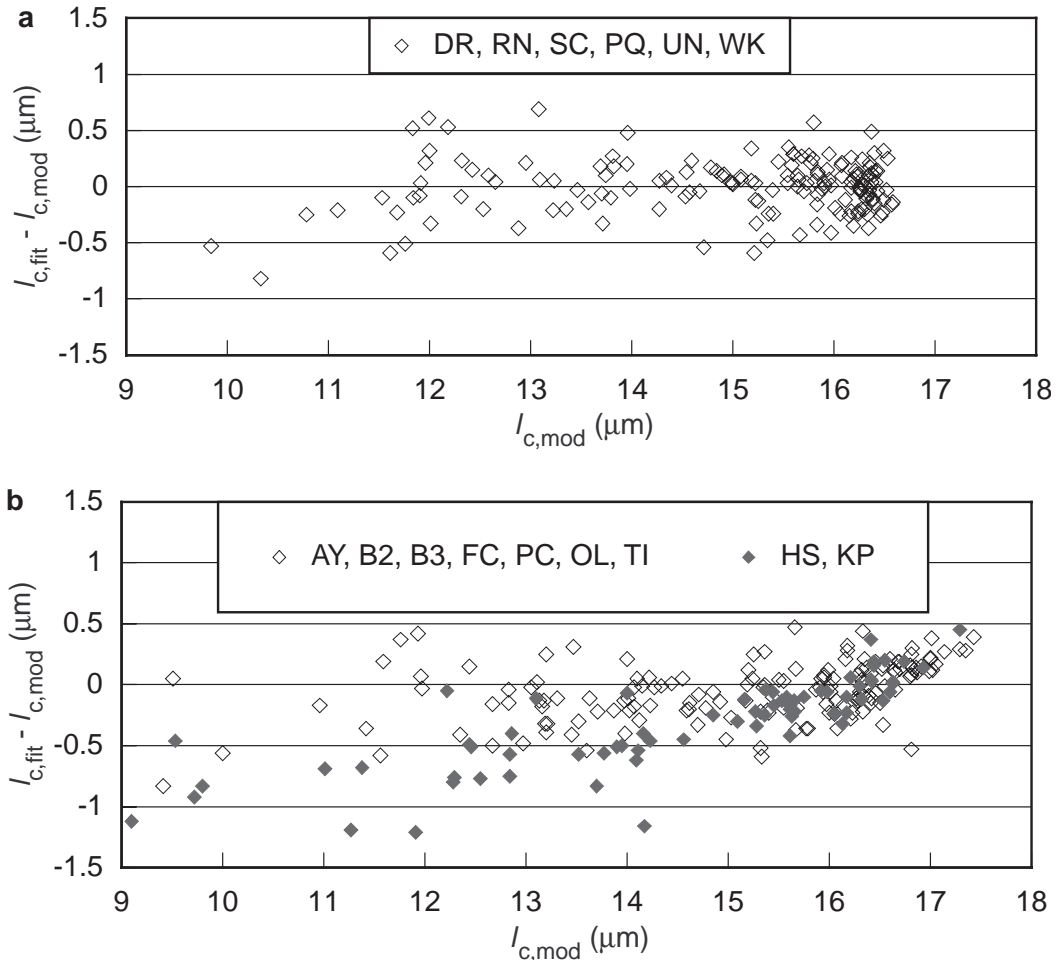


**FIGURE 8.** Residuals of fitted vs. mean *c*-axis projected fission-track lengths (**a**) for six selected apatites, and (**b**) for remaining apatites.

dent upon the crystallographic orientation of the track. Relative frequency of fission-track length measurement is plotted against track angle to the crystallographic $c$ axis in Figure 10 for four apatites (B3, DR, HS, and RN; Carlson et al., 1999, this volume; only those experiments lacking evidence of accelerated length reduction are considered). It is apparent in Figure 10 that fission tracks oriented at between ~65–75° to the $c$ axis are more likely to be observed than their counterparts at other orientations, even though the mean fission-track length at lower angles to the $c$ axis is always significantly greater. This effect is likely the result of anisotropic etching characteristics (e.g., $D_{par} > D_{per}$ in all cases; Table 1), which give rise to narrow widths of etched fission tracks at low and very high angles to the crystallographic $c$ axis and a consequent lack of fully etched fission tracks in those orientations.

### Fission-track length vs. fission-track density

The $c$-axis projection model presented here can be used to examine the relationship between fission-track length and fission-track density as observed by Green (1988). Using the set of ellipses and line segments defined by Equations 1 through 3, combined with a number of assumptions about observational biases, it is possible to construct a theoretical relationship between observed length and density that can be compared to the experimental data.
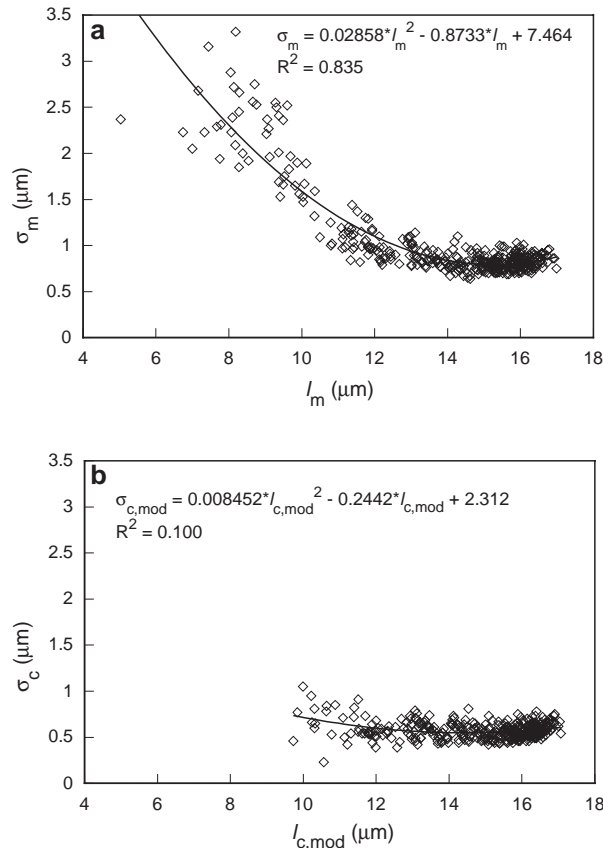
To calculate a mean fission-track length for a single population, it is necessary to begin with the assumption that fission tracks are equally likely to exist in any angular orientation in the horizontal plane. For fission-track populations that lack evidence of accelerated length reduction, the "observed mean" for the population is equated to the weighted mean radius of the $c$-axis projection model. The weighting factor for the radius at each angular orientation is obtained from a smoothed observational bias function, similar to that presented in Figure 10, developed for the six selected apatites. For fission-track populations that exhibit evidence of accelerated length reduction, the "observed mean" for the population is the weighted mean value of a sum of a Gaussian curve with standard deviation of 1.0 μm about the radius of the $c$-axis projection model with the weighting factor for each discrete value set proportional to the value itself. An additional important condition is applied that there is a minimum observable fission-track length below which the probability of observation equals zero. If a portion of a population falls below this limit, an additional weighting factor is calculated to account for the missing tracks, and a revised mean is calculated based on those that remain.

Estimating fission-track density requires taking into account the three-dimensional distribution of track lengths that might intersect a polished surface and the proportion of those tracks that would be counted. This distribution is estimated by first rotating the curve that describes the population around the $c$ axis, creating an ellipsoid (examples of these curves are plotted in Fig. 7). If the curve includes a line segment representing accelerated length reduction, the ellipsoid is pinched around its equator. The different fission-track lengths along the curve are then weighted by the amount of area their respective three-dimensional angular intervals subtend on a unit sphere. The probability of a track impinging the surface is assumed to be proportional to its length, and it is assumed that a track must have at least 1.5 μm of length inside the polished surface to be counted.
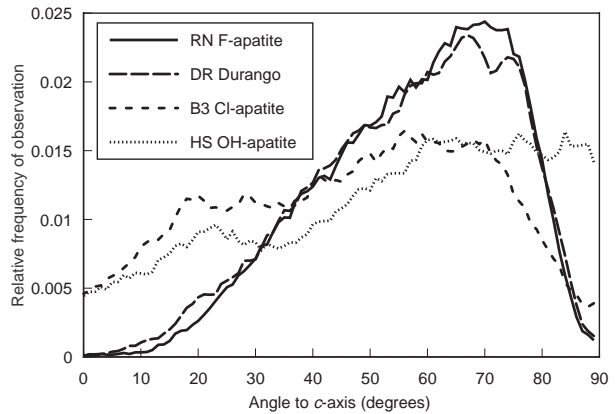


**FIGURE 9.** (**a**) Plot of $\sigma_m$ vs. $l_m$ for all 387 experiments Carlson et al. (1999, this volume). (**b**) Plot of $\sigma_{c,mod}$ vs. $l_{c,mod}$ for all 387 experiments.



**FIGURE 10.** Relative frequencies of observation vs. fission-track angle to the crystallographic $c$ axis for apatites B3, DR, HS, and RN from the experiments of Carlson et al. (1999, this volume). All individual experiments for each apatite sample have been combined to create each respective frequency curve and only those experiments lacking evidence of accelerated length reduction are included.

It should be noted that some of the above assumptions are quite simplified, and they may be replaced by more complex treatments. For example, the sharp length cutoffs below which fission tracks cannot be measured or counted could be replaced by gradual functions. Experimentally constraining such relationships is not practical using the current data set, however, and it is likely that the values for the cutoffs used here provide adequate estimates.

Figure 11 shows the estimated relationship between observed mean length and density compared to the data presented by Green (1988) for DR and RN apatites, these apatites being common to the current study and that of Green (1988). The correspondence is remarkable, and serves as an additional verification of the underlying soundness of the $c$ axis-projection model. In the upper-right part of the diagram, it is interesting to note that it is only because of the angular biasing correction based on Figure 10 that the initial part of the line relating observed mean length to measured density follows a 1:1 trend. If length biasing alone were responsible, the relation would tend towards higher observed mean lengths, as observation in two dimensions overweights tracks with low angles to the $c$ axis relative to their actual proportion in three dimensions.

### Anisotropy of natural fission tracks in apatite

Ellipses have been fit to 390 natural fission-track length populations measured from a wide variety of samples. Fitted values of $l_a$ are plotted against $l_c$ for all 390 fission-track length populations in Figure 12. Equation 1, which relates these parameters for the six selected apatites, is superimposed on that diagram. Interestingly, the natural data define a fairly tight trend that overlaps but is shifted somewhat away from the trend defined by the experimental data of Carlson et al. (1999, this vol-

ume). The cause of this shift is unclear but it may be due, in part, to the comparison of ellipses fitted to a spectrum of fission-track length populations (i.e., natural fission-track data) vs. ellipses fitted to single fission-track length populations (i.e., the laboratory fission-track data). Importantly, all of the natural data plotted in Figure 12 were obtained using [252]Cf-irradiated grain mounts whereas most of the experimental data were obtained using non-[252]Cf-irradiated grain mounts. The most likely source of the divergence between the natural and experimental data trends is that [252]Cf-irradiation may obscure the true direction of the crystallographic $c$ axis of an apatite grain. Natural apatite grains are commonly anhedral and well-rounded, or fragments of larger grains, and thus may not preferentially have their c-axes in the plane of the microscope stage. Due to the nearly vertical incidence angle of the [252]Cf-fission-fragment tracks in [252]Cf-irradiated grains, it may be inappropriate to rely solely upon the parallel orientation of fission-track etch pits as an indicator of $c$-axis orientation, as was done for the natural data plotted in Figure 12. It is expected that an analysis that incorporates some uncertainty regarding $c$-axis direction will plot somewhere between the experimentally determined line and 1:1 relationship, in a manner similar to the natural data in Figure 12.

The fact that the natural data in Figure 12 relate in an understandable and expected way to the experimental data trend is taken as evidence that the process responsible for fission-track length anisotropy in the laboratory is operative in the geological environment as well, and that the $c$-axis projection model presented here can be applied confidently to natural fission-track length populations. However, it is clear that this issue needs further study and caution is recommended concerning the determination of the $c$-axis direction in [252]Cf-irradiated grain mounts.
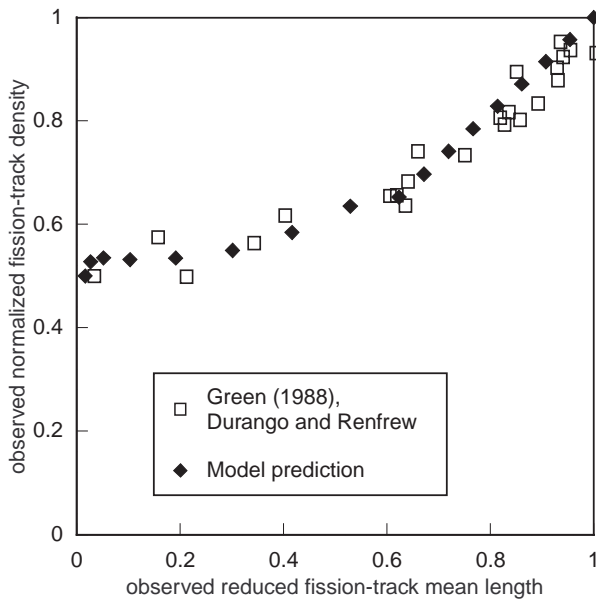


**FIGURE 11.** A plot of reduced fission-track density vs. reduced mean fission-track length comparing the experimental data of Green (1988) to the predictions of the model presented here.
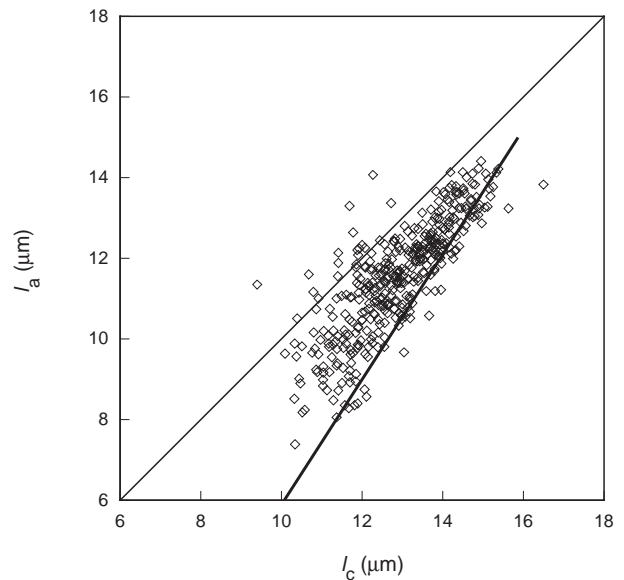


**FIGURE 12.** Plot of $l_a$ vs. $l_c$ for 390 natural fission-track populations.

## Other orientation-dependent considerations

An important implication of Equation 2 is that there is no departure from the elliptical model for fission tracks oriented parallel to the crystallographic c axis. Thus, the process that is responsible for accelerated length reduction of fission tracks at relatively high angles to the c axis does not affect tracks at low angles to the c axis. Furthermore, the final stage of annealing of fission tracks oriented nearly parallel to the c axis is sudden.

Other investigators have documented features in apatite related to fission tracks, crystallographic orientation, or both that may have relevance regarding the actual physical process(es) by which fission tracks anneal in apatite. Most notably, apatite exhibits uniaxial optical anisotropy (e.g., Klein and Hurlbut 1985). Elliptical-model fission tracks in apatite describe a mean-length fission-track surface that is directly analogous to the uniaxial optical indicatrix of apatite. Additionally, Paul and Fitzgerald (1992, their Fig. 5) show a fission track with a cross-section that exhibits hexagonal symmetry oriented parallel to the c axis. These authors argue that the cross-sectional geometries of fission tracks oriented in other crystallographic directions reflect the respective symmetries in those directions as well. It appears that, at least under an electron beam, these fission tracks have attained a minimum interfacial surface energy configuration spontaneously. If such behavior occurs in apatites not subjected to electron bombardment, the initial realization of this minimum interfacial surface energy configuration may account for the room-temperature annealing of fission tracks observed by Donelick et al. (1990).

According to Wulffs theorem of crystal growth (e.g., Doremus 1985, p. 39), surfaces with relatively low interfacial surface energies grow more slowly than surfaces with relatively high interfacial surface energies. Apatite, which typically exhibits c-axis parallel prismatic crystal habit, exhibits higher crystal growth rates on surfaces oriented perpendicular to the c axis vs. surfaces oriented parallel to the c axis. Furthermore, prismatic and pyramidal faces are commonly well developed on apatite crystals whereas basal faces are typically not well developed. Watson et al. (1985, their Fig. 6) observed that polished crystallographic planes perpendicular to the c axis (i.e., parallel to basal crystal faces) became rough when heated in a silicate melt whereas crystallographic planes parallel to the c axis (i.e., parallel to prismatic crystal faces) remained smooth. It may be that fission tracks, once they attain their minimum interfacial surface energy configuration, experience some degree of roughening of their sides. For tracks oriented perpendicular to the c axis, the fission-track sides may experience the greatest degree of roughening; at high degrees of annealing, the roughening may be so severe as to cause the accelerated length reduction discussed above. On the other hand, fission tracks oriented parallel to the c axis would not experience any surface roughening and therefore would not exhibit accelerated length reduction.

## CONCLUSIONS

Based on fission-track annealing data obtained for five calcian fluorapatites and Durango apatite, the elliptical model of Donelick (1991) has been reaffirmed and extended to all degrees of annealing including fission-track populations that have experienced accelerated length reduction. The resulting fission-track length c-axis projection model removes much of the increased fission-track length variance associated with highly annealed fission-track populations. Natural fission-track populations exhibit a track-length anisotropy trend that overlaps but is shifted somewhat relative to that observed for the experimental data. The observation that the natural and experimental trends relate to one another in an understandable way is taken as evidence that the process responsible for fission-track length anisotropy in the laboratory is operative over geological time scales as well. As such, the c-axis projection model presented here can be applied with confidence to natural fission-track populations. However, caution is recommended concerning the determination of the c-axis direction in $^{252}$Cf-irradiated grain mounts.

Fission-track length observational bias is found to vary significantly with crystallographic orientation, with tracks oriented between ~65–75° being most likely to be observed and measured in c-axis parallel crystallographic planes. Using this information, the c-axis projection model developed here, and several reasonable simplifying assumptions, it is possible to match closely published experimental data concerning the relationship between fission-track length vs. fission-track density.

## REFERENCES CITED

Burtner, R.L., Nigrini, A., and Donelick, R.A. (1994) Thermochronology of Lower Cretaceous source rocks in the Idaho-Wyoming thrust belt. American Association of Petroleum Geologists Bulletin, 78, 1613–1636.
Carlson, W.D. (1990) Mechanisms and kinetics of apatite fission-track annealing. American Mineralogist, 75, 1120–1139.
Carlson, W.D., Donelick, R.A., and Ketcham, R.A. (1999) Variability of apatite fission-track annealing kinetics I: Experimental results. American Mineralogist, 9, 1213–1223.
Corrigan, J.D. (1991) Inversion of apatite fission-track data for thermal history information. Journal of Geophysical Research, 96, 10347–10360.
Crowley, K.D. (1993) LenModel: a forward model for calculating length distributions and fission-track ages in apatite. Computers and Geosciences, 19, 619–626.
Crowley, K.D., Cameron, M., and Schaeffer, R.L. (1991) Experimental studies of annealing of etched fission tracks in fluorapatite. Geochimica et Cosmochimica Acta, 55, 1449–1465.
Donelick, R.A. (1991) Crystallographic orientation dependence of mean etchable fission track length in apatite: An empirical model and experimental observations. American Mineralogist, 76, 83–91.
——(1993) A method of fission track analysis utilizing bulk chemical etching of apatite. U.S. Patent Number 6,267,274.
——(1995) A method of fission track analysis utilizing bulk chemical etching of apatite. Australian Patent Number 658,800.
Donelick, R.A., Roden, M.K., Mooers, J.D., Carpenter, B.S., and Miller, D.S. (1990) Etchable length reduction of induced fission tracks in apatite at room temperature (~23°C): Crystallographic orientation effects and "initial" mean lengths. Nuclear Tracks and Radiation Measurements, 17, 261–267.
Doremus, R.H. (1985) Rates of Phase Transformations, 176 p. Academic Press, Orlando, Florida.
Green, P.F. (1988) The relationship between track shortening and fission track age reduction in apatite: Combined influences of inherent instability, annealing anisotropy, length bias and system calibration. Earth and Planetary Science Letters, 89, 335–352.
Green, P.F., Duddy, I.R., Gleadow, A.J.W., Tingate, P.R., and Laslett, G.M. (1986) Thermal annealing of fission tracks in apatite 1. A qualitative description. Chemical Geology, Isotope Geoscience Section, 59, 237–253.
Green, P.F., Duddy, I.R., Laslett, G.M., Hegarty, K.A., Gleadow, A.J.W., and Lovering, J.F. (1989) Thermal annealing of fission tracks in apatite 4. Quantitative model-

ling techniques and extension to geological timescales. Chemical Geology, Isotope Geoscience Section, 79, 155–182.

Ketcham, R.A., Donelick, R.A., and Carlson, W.D. (1999) Variability of apatite fission-track annealing kinetics III: Extrapolation to geological time scales. American Mineralogist, 9, 1235–1255.

Klein, C. and Hurlbut, C.S. (1985) Manual of Mineralogy. 20th Edition, 596 p. John Wiley and Sons, New York.

Laslett, G.M., Kendall, W.S., Gleadow, A.J.W., and Duddy, I.R. (1982) Bias in measurement of fission-track length distributions. Nuclear Tracks, 6, 79–85.

Laslett, G.M., Green, P.F., Duddy, I.R., and Gleadow, A.J.W. (1987) Thermal annealing of fission tracks in apatite 2: A quantitative analysis. Chemical Geology, Isotope Geoscience Section, 65, 1–13.

Paul, T.A. and Fitzgerald, P.G. (1992) Transmission electron microscopic investigation of fission tracks in fluorapatite. American Mineralogist, 77, 336–344.

Press, W.H., Flannery, B.P., Teukolsky, S.A., and Vetterling, W.T. (1986) Numerical Recipes, 818 p. Cambridge University Press, Cambridge, England.

Watson, E.B., Harrison, T.M., and Ryerson, F.J. (1985) Diffusion of Sm, Sr, and Pb in fluorapatite. Geochimica et Cosmochimica Acta, 49, 1813–1823.

Willett, S.D. (1997) Inverse modeling of annealing of fission tracks in apatite 1: A controlled random search method. American Journal of Science, 297, 939–969.